

RESEARCH PAPER

Antibacterial Response of Cd-TiO₂/PEG/folic acid Nanocomposite under Ultraviolet, Visible light, or Ultrasonic Irradiation

Sanaz Naghibi^{1*}, Mehrnaz Gharagozlou² and Shohreh Vahed³

¹ Department of Materials Engineering, Shahreza Branch, Islamic Azad University, Shahreza, Iran

² Department of Nanomaterials and Nanocoatings, Institute for Color Science and Technology, Tehran, Iran

³ Department of Food Science, Shahreza Branch, Islamic Azad University, Shahreza, Iran

ARTICLE INFO

Article History:

Received 11 June 2019

Accepted 19 August 2019

Published 01 October 2019

Keywords:

Antibacterial Performance

Biomaterials

Cd-Doped TiO₂ NPs

Cd-TiO₂/PEG/FA

Nanocomposite

Folic Acid

ABSTRACT

Synthesis and characterization of Cd-TiO₂/PEG/FA nanocomposite as a biomaterial is the main aim of this research. Cd-doped TiO₂ nanoparticles (NPs) were synthesized by solvothermal assisted sol-gel method. Then, polyethylene glycol (PEG) was added to the as-synthesized NPs to modify their surface and to prevent agglomeration. In the next step, folic acid (FA) was conjugated to Cd-TiO₂/PEG nanocomposite. Optimization of FA concentration and influence of ultraviolet (UV) radiation, visible light, or ultrasonic irradiation on antibacterial activity of the synthesized nanocomposite were assessed. Results showed that the influence of FA on the antibacterial performance of the as-synthesized compounds is positive and dose-dependent. FA was used as bait for bacteria and led them to accumulate around the Cd-TiO₂ NPs. The bactericidal response under UV or visible light irradiation was maximized at 0.6 weight ratio of FA to Cd-TiO₂, whereas, this parameter under ultrasonic irradiation was improved and then became approximately constant.

How to cite this article

Naghibi S, Gharagozlou M, Vahed S. Antibacterial Response of Cd-TiO₂/PEG/folic acid Nanocomposite under Ultraviolet, Visible light, or Ultrasonic Irradiation. J Nanostruct, 2019; 9(4): 768-775. DOI: 10.22052/JNS.2019.04.018

INTRODUCTION

Microorganisms or microbes are described as microscopic organisms which can be survived everywhere. Although some of them are beneficial for the environment, animals, and plants [1], most of the diseases originate from the microbes via toxins propagation in foods and water sources [2]. Traditional disinfection methods produce harmful wastewater or byproducts and are expensive. On the other hand, the use of antibiotics in food-producing industry causes antibiotic resistance [3]. Recently, new materials have been developed to deal with these problems. Some of the metallic and ceramic semiconductors are of the modern disinfectants which can degrade or prevent growth and proliferation of microbes. Ag-containing composites and ZnO NPs are two

famous and popular compounds to defeat cancer cells, bacteria, and infected cells. It is suggested that their toxicity originates from the disruption of ion homeostasis and/or cell wall-damaging [4, 5]. TiO₂-containing NPs or nanohybrids are the other worth and mostly applied materials due to their microbicidal activity. This performance is a result of activation of semiconductor compound and generation of charge carriers. TiO₂ NPs have two prominent characteristics. (i) These NPs are active against several types of microorganisms, such as Gram-positive and negative-bacteria, fungi, etc. (ii) TiO₂-containing nanohybrids are not toxic and their biocidal performance is a non-contact action [6]. The possible performances of UV-activated TiO₂-containing compounds are being extensively

* Corresponding Author Email: naghibi@iaush.ac.ir

used to oxidize and/or degrade microorganisms [7-9]. However, these systems require UV-irradiation at high intensity; so their applications are restricted. Tackling this problem is possible by (i) decreasing the band gap energy (E_g), and/or (ii) using other activation methods.

TiO₂ doping with metallic ions could lead to decrease E_g and is taken into consideration. Some of the most popular dopants that are intended to modify TiO₂ NPs include Fe [10, 11], Ag [12], and Cu [13].

Recently, the influence of different metallic dopants on TiO₂ NPs has been investigated elsewhere. Correspondingly, among Cd, Ag, Fe, Ce, and Cu, only Cd and Ag could improve absorbance of UV-visible light. On the other hand, both of them are induced by sonoirradiation [14]. Considering the interesting results in the previous studies, we have decided to investigate the antimicrobial behavior of Cd-TiO₂ compound under different irradiation sources.

Another point that should be considered is the tendency of NPs to be agglomerated and precipitated in a suspension. This phenomenon causes to decrease the performance of NPs. The surface covering of NPs with a polymeric compound (such as PEG) is a way to deal with this problem. Microorganisms need folate species to be alive. This characteristic has been used to design smart materials [15-17].

In this work, Cd-doped TiO₂ NPs were synthesized by sol-gel / solvothermal method to achieve NPs with high specific surface area and uniformity. PEG was loaded on the as-synthesized NPs to avoid agglomeration and sedimentation. Then, folic acid was added to Cd-TiO₂/PEG compound and subsequently, the microbicidal performance of the Cd-TiO₂/PEG/FA nanocomposite was assayed under UV-, visible-, and sonoirradiation. This was investigated to evaluate the possibility of using Cd-TiO₂/PEG/FA nanocomposite (Cd-TiO₂ NPs to provide sono- or photo-activity, PEG to avoid sedimentation, and FA to increase the vicinity of nanoparticles and bacteria) in an antibacterial application. Although using folic acid promotes the anticancer performance of nanoparticles in photodynamic therapy due to the folate receptors, the influence of using this inorganic compound on the antibacterial performance of a photocatalyst would be studied for the first time.

MATERIALS AND METHODS

Starting chemicals

Titanium isopropoxide (TTIP, Ti(OCH(CH₃)₂)₄) as Ti-containing precursor, cadmium nitrate

tetrahydrate (Cd(NO₃)₂·4H₂O) as Cd-containing precursor, isopropyl alcohol (iPrOH, C₃H₈O, >99.5%) as solvent, nitric acid (HNO₃, 65%) as pH adjusting agent, deionized water as hydrolytic agent, polyethylene glycol (PEG, 6000 g/mol), and folic acid (FA) were purchased from Merck® (Frankfurt, Germany) and used as starting materials.

N,N'-dicyclohexyl carbodiimide (DCC, >99%) and dimethyl sulfoxide (DMSO, 99%) were utilized for FA activation process.

Preparation of Cd-doped TiO₂ NPs

The Cd-doped TiO₂ NPs were synthesized by solvothermal assisted sol-gel method. Preparation parameters have been optimized to reach the highest sonocatalytic performance. For this reason, TTIP, iPrOH, distilled water, and nitric acid were mixed with the molar ratio of 2.8, 9.2, 166.7, and 1.0, respectively. The obtained solution was relaxed for 24 h to achieve a white sediment. Then, 1 g of the dried sediment powder, 0.063 mmol of Cd-containing precursor, 7.5 mL of water, and 59 mL of iPrOH were mixed and stirred for 24 h to achieve a homogenous solution. The obtained solution was then treated via a solvothermal process at 200 °C for 8 h to precipitate some colored particles. This sample is named as Cd-TiO₂.

Functionalization of Cd-TiO₂ NPs by PEG

PEG was used as the functionalization agent and conjugated to Cd-TiO₂ NPs. For this aim, adequate amounts of the as-synthesized NPs and distilled water were mixed to reach the concentration of 1 g/L and sonicated for 2 h to deagglomerate the NPs before PEG addition. Then, 0.2 g of PEG was added and mixed with 100 mL of the Cd-TiO₂ solution and sonicated for 3 h. This sample is named as Cd-TiO₂/PEG nanocomposite.

Conjugation of FA to Cd-TiO₂/PEG

In this step, Cd-TiO₂/PEG nanocomposite and FA should be conjugated. Generally, covalent bonding between FA molecules and NPs could not form directly. FA needs an activation process to form isourea via carboxyl group activation. This procedure has been reported in detail elsewhere [18]. For this reason, FA was solved in DMSO with equal weight ratio. Then DCC was added to the solution under N₂ gas flow and stirred for 2 h. Subsequently, Cd-TiO₂/PEG nanocomposite powder was added to the obtained solution and stirred under N₂ atmosphere for 2 h. The as-

modified NPs were separated from the solution by a freeze-dryer (Christ, Germany). This sample is named as Cd-TiO₂/PEG/FA nanocomposite. The weight ratio of FA to Cd-TiO₂ NPs should be optimized; therefore, four weight ratios (0.2, 0.4, 0.6, and 0.8) were incorporated. The schematic flowchart of the mentioned synthesis procedures is shown in Fig. 1.

Characterization

The as-synthesized samples were characterized using X-ray diffractometry (XRD, D8 Advance, Bruker) with a Co X-ray tube, transmission electron microscopy (TEM, LEO 912 AB), diffuse reflectance spectroscopy (DRS, UV-visible scanning spectrophotometer), and Fourier transform infrared spectroscopy (FTIR, PerkinElmer).

Tauc plot was drawn between $(\alpha hu)^2$ vs. hu (where α and hu are absorption coefficient and photon energy, respectively) to measure the optical band gap energy (E_g) [19].

The concentration of the Cd in TiO₂ structure was determined by atomic absorption spectroscopy (AAS) using an Analyst 300 spectrophotometer (Perkin-Elmer, USA).

The antibacterial activity of the samples under ultrasonic, UV or visible light irradiation was determined against facultative Gram-negative *Escherichia coli* (*E. coli* - ATCC 43886). Preparation

of the bacteria-containing solution has been explained elsewhere [10]. For this reason, *E. coli* was precultured in nutrient agar (NA) medium at ~ 37 °C for 24 h. The treated cells were then diluted and re-suspended with phosphate buffer solution (PBS) to 2.5–10 × 10⁵ colony forming units per mL (CFU/mL). Using the surface plate method, 200 μL of the bacterial solutions and 1 μL of the samples suspension with a concentration of 10 g/L were mixed and then exposed to irradiation for 5 h. Three types of irradiation sources were used:

- UV irradiation by two UV lamps (365 nm, 15 W),
 - Visible light by two fluorescent lamps (18 W)
 - Ultrasonic irradiation by an ultrasonic bath at 37 kHz frequency and 90 W output power
- After irradiation, two techniques were applied to evaluate the bactericidal responses of the samples:
- Counting the numbers of surviving bacteria for the samples irradiated with UV or visible light.
 - Measuring the non-growth halo diameter for the samples irradiated with ultrasonic waves.

RESULTS AND DISCUSSION

XRD, DRS, AAS, and TEM results

Fig. 2-A shows XRD patterns of the as-synthesized Cd-TiO₂ and TiO₂-P25 NPs. The obtained results approved the formation of

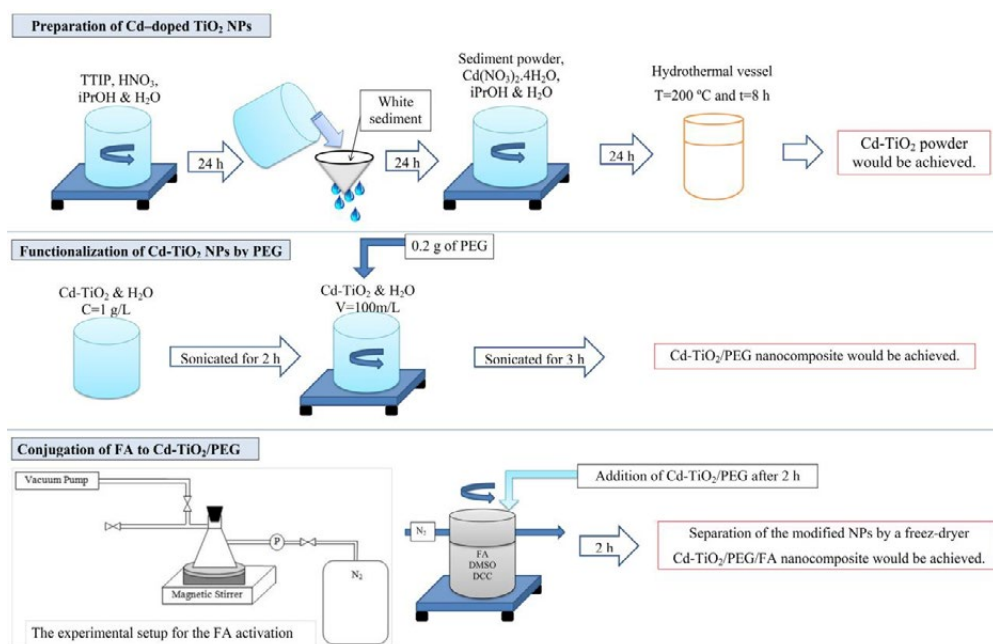


Fig. 1. The schematic flowchart of the synthesis procedures

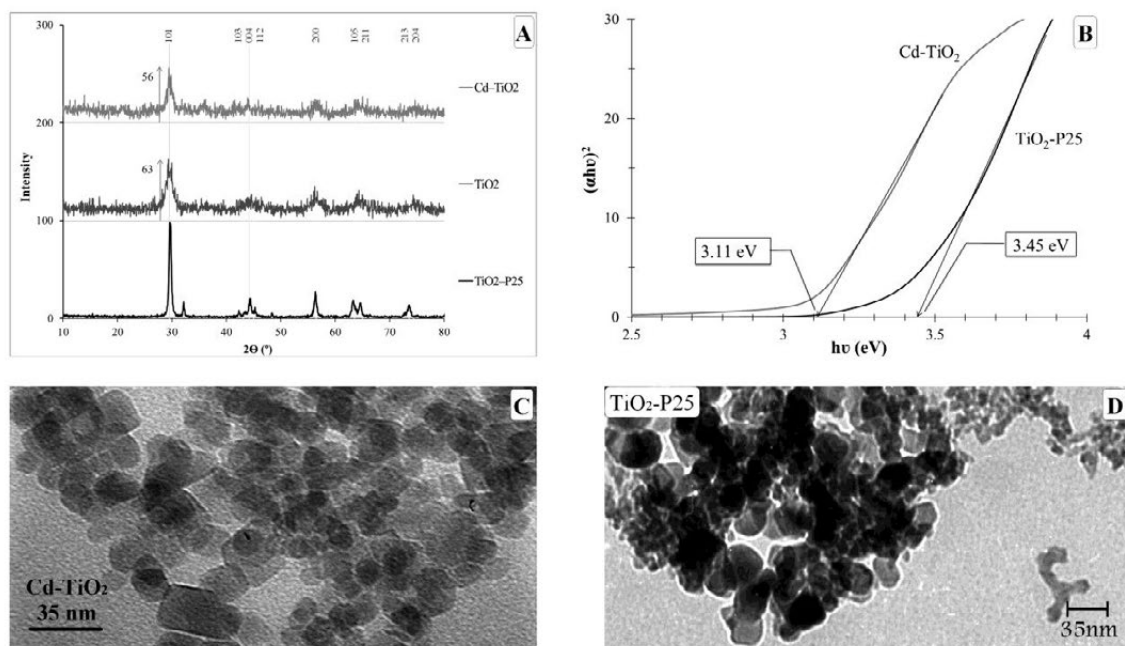


Fig. 2. (A): XRD patterns of the as-synthesized Cd-TiO₂, TiO₂, and TiO₂-P25 NPs, (B): DRS results for the as-synthesized Cd-TiO₂ and TiO₂-P25 NPs, (C): TEM image of the as-synthesized Cd-TiO₂ NPs, and (D): TEM image of TiO₂-P25 NPs.

anatase [PDF No.: 4-477] in pristine TiO₂ and also Cd-TiO₂ samples. The intensity of the main peak of anatase which is located at $2\theta=30^\circ$ is considered as an index to compare the as-synthesized powder and commercial TiO₂-P25 powder. It is clear that the height of this peak was about 56 and 63 for Cd-TiO₂ and TiO₂, respectively, which are less than that of TiO₂-P25. This can be related to the smaller NPs and/or lower degree of crystallinity in both synthesized samples in comparison to the commercial TiO₂-P25 powder. On the other hand, dopants cause a structural change in their matrix. The type and intensity of the changes are related to three items; amounts, ionic radii, and electrical charge of the dopants. Referring to the AAS results, the amount of Cd which is doped into TiO₂ structure has been measured about 0.59 wt. %. Since the measured value is very close to the theoretical value (i.e. 0.710 wt.%), Cd could be considered as the source of the mentioned changes in TiO₂ structure [14].

Based on Fig. 2-B, E_g value of the as-synthesized sample was ~ 3.11 eV, which is less than that of TiO₂-P25, 3.45 eV. It means that Cd-doping led to decrease band gap of TiO₂ structure and its photocatalytic activity needs less energy. TEM images of the Cd-TiO₂ and TiO₂-P25 samples are illustrated in Fig. 2-C and 2-D, respectively. It is

clear that the as-synthesized NPs have a uniform shape and particle size about 10–20 nm. This observation is in good agreement with XRD peaks intensity.

FTIR results

The next step in this research was to consider the dispersion state and sedimentation behavior of the as-synthesized NPs. To improve the performance of the Cd-TiO₂ NPs, they should be modified by organic molecules [20]. For this aim, PEG was selected as a modification agent. After that, FA was conjugated to the as-prepared compound to enhance its antibacterial performance [21]. FTIR analysis was utilized to evaluate bonding formation between Cd-TiO₂ NPs, PEG, and FA molecules. The resulted spectra are illustrated in Fig. 3 and assignments of the bands are presented in Table 1. According to the first row of Table 1 (Cd-TiO₂), the vibration at 400–800 cm⁻¹ was assigned to metal oxides (Ti–O and/or Cd–O) bands [22]. The vibrations at the range of 1000–2000 cm⁻¹ may be related to residual raw materials in the synthesis procedure of Cd-TiO₂. The vibration at ~ 3500 cm⁻¹ was assigned to O–H groups [23]. According to the second row of Table 1 (Cd-TiO₂/PEG), the vibration at ~ 700 cm⁻¹ may be related to Ti–O and/or Cd–O band. The vibrations at 1325, 1455, and 2910 cm⁻¹

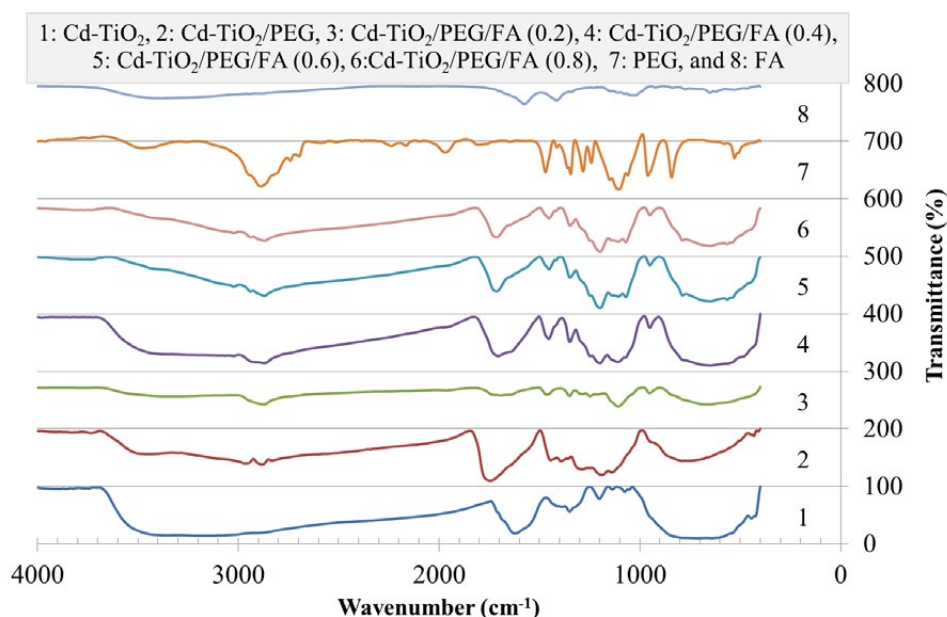


Fig. 3. FTIR spectra of (1): Cd-TiO₂, (2): Cd-TiO₂/PEG, (3): Cd-TiO₂/PEG/FA (0.2), (4): Cd-TiO₂/PEG/FA (0.4), (5): Cd-TiO₂/PEG/FA (0.6), (6): Cd-TiO₂/PEG/FA (0.8), (7): PEG, and (8): FA. The assignments of the bands are presented in Table 1.

Table 1. Assignment of FTIR spectra of the as-synthesized samples, pristine PEG, and pristine FA.

No.	Sample	IR bands (cm ⁻¹)	Description	Ref.
1	Cd-TiO ₂ NPs	400-800	Ti-O	[22]
		1222	δ (C-O)	
		1362	ν (C-H)	
		1650	ν (C=C)	
2	Cd-TiO ₂ /PEG	~3500	ν (O-H)	
		~700	Ti-O	
		1220	δ (C-O)	
		1325	δ (-CH ₂)	
		1455	δ (-CH)	
		1777	ν (C=O)	
		2910	ν (C-H) / ν (C=C)	
3	Cd-TiO ₂ /PEG/FA (0.2)	3540	ν (O-H)	
		400-800	Ti-O	
4	Cd-TiO ₂ /PEG/FA (0.4)	960	δ (-CH) out-of-plane	
		1150	ν (C-O-C) ether vibration	
5	Cd-TiO ₂ /PEG/FA (0.6)	1225	δ (C-O)	
		1360	ν (C-H)	
6	Cd-TiO ₂ /PEG/FA (0.8)	1480	δ (-CH)	
		1740	ν (C=O)	
7	PEG	2900	ν (C-H) / ν (C=C)	[18, 25]
		3500	ν (O-H)	
8	FA	535	ν (C=O)	[26]
		848	δ (-CH ₂)	
		961	δ (-CH) out-of-plane	
		1126	ν (C-O)	
		1242	δ (-CH ₃)	
		1282	δ (-CH ₃)	
		1344	δ (-CH ₂)	
		1471	δ (-CH)	
		1642	ν (C=O)	
		2884	ν (C-H)	
8	FA	3500	ν (O-H)	[26]
		660	ν (C=O)	
		1062	ν (C-O-C)	
		1426	OH deformation band	
		1584	ν (N-H)	
		3482	ν (O-H)	

ν: Stretching vibration, δ: bending vibration

Table 2. The survival rate of *E. coli* treated with the as-synthesized samples exposed under UV, visible light, and ultrasonic irradiation compared with a blank sample.

No.	Sample	UV irradiation		Visible light irradiation		Ultrasonic irradiation
		Count (*10 ⁶)	Log of reduction	Count (*10 ⁶)	Log of reduction	Non-growth halo diameter (mm)
1	Cd-TiO ₂ NPs	0.050	2.0	0.200	1.4	4
2	Cd-TiO ₂ /PEG	0.010	2.7	0.100	1.7	5
3	Cd-TiO ₂ /PEG/FA (0.2)	0.010	2.7	0.050	2.0	8
4	Cd-TiO ₂ /PEG/FA (0.4)	0.005	3.0	0.010	2.7	9
5	Cd-TiO ₂ /PEG/FA (0.6)	0.003	3.2	0.005	3.0	10
6	Cd-TiO ₂ /PEG/FA (0.8)	0.006	2.9	0.012	2.6	10
7	Blank	5.000	-	5.000	-	-

were related to the existence of PEG (see 6th row in Table 1). Moreover, some peaks were observed in Cd-TiO₂/PEG pattern which is seen neither in the Cd-TiO₂ sample nor in the PEG spectrum. One of these vibrations was located at 1777 cm⁻¹. This new band confirmed the formation of conjugation between Cd-TiO₂ NPs and PEG molecules. The mentioned vibration in functional group region ascribes a functional group containing a carbonyl (C=O). According to the third to sixth rows of Table 1 (Cd-TiO₂/PEG/FA), in addition to the vibrations which are related to Cd-TiO₂ NPs (400-800 cm⁻¹) and PEG (960, 1480 and 2900 cm⁻¹), some new bands appeared in these spectra at 1150, 1225, and 1360 cm⁻¹, which are related to C–O–C, C–O, and C–H vibrations, respectively. These are not basically matched with FA vibrations (see 8th row). It seems that the nonexistence of the FA vibrations in these spectra is related to the low intensity of FA vibrations in comparison to other peaks. On the other hand, the as-formed bands confirmed the formation of bonding between Cd-TiO₂/PEG and FA. Accordingly, an acceptable synthesis method was utilized to loading of FA and PEG on the Cd-TiO₂ NPs.

Improvement in the bactericidal response of Cd-TiO₂/PEG/FA compound under visible light, UV, or ultrasonic irradiations

Bactericidal assays were performed to compare the effects of PEG and FA loading on the Cd-TiO₂ NPs under different irradiations. Table 2 represents the results of antibacterial screening under visible light, UV, or ultrasonic irradiations, showing a decrease in *E. coli* survivability due to the modification process. In the blank and Cd-TiO₂ samples under different irradiations, the viabilities of bacteria decreased due to the existence of the photocatalyst NPs; therefore, the main role of bacterial-killing under UV light,

visible light, or ultrasonic waves accomplished by photo/sono-activation of the NPs (no irradiation). As can be seen, Cd-TiO₂/PEG powder exhibited relatively higher bactericidal effect compared to Cd-TiO₂ powder when exposed to three sources of irradiations. Under UV irradiation, the synthesized Cd-TiO₂ powder destroyed 2.0 log concentrations of bacteria, while only 1.4 log were killed under visible light. This event is possibly relates to:

1. UV is known as a disinfection agent. It can destroy the nucleic acid of a bacterium and consequently leads to not perform vital cellular tasks and to lose its reproductive capability.

2. The lower concentration of the as-formed OH radicals by the semiconductor under visible light in comparison to the UV irradiation.

However, similar different results were obtained in other samples when the targets were irradiated with UV or visible light. Measurement of bactericidal effect under ultrasonic irradiation was accomplished via a different method; therefore, the comparison between these results and UV/visible light irradiated samples cannot be correct.

Antibacterial performance of Cd-TiO₂ NPs was improved by PEG addition under UV, visible or ultrasonic irradiation. There is an energy gap in a semiconductor material. A source of energy is required to overcome this gap. When a semiconductor is irradiated, if the provided energy is equal to or higher than that of the band gap, the excitation process could occur and superoxide and peroxide radicals would form. These radicals are effective in destroying bacteria [10]. In this process, the free surface of NPs is important and determinative. The NPs tend to form aggregates, decreasing their free surface and deteriorating the surface-dependent properties. Addition of PEG to the NPs led to decrease agglomeration by covering their surfaces [20]. This phenomenon led to improving photo and sono-activity of the Cd-TiO₂/

PEG compound in comparison to the Cd-TiO₂ NPs.

Folic acid is essential for microorganisms to secrete the nucleic acid that makes up their DNA. This characteristic can be a reason for the accumulation of bacteria around folate derivatives biomaterials [24].

To evaluate this supposition, Cd-TiO₂/PEG/FA compounds were prepared and their antibacterial performances with different amounts of FA were compared under UV, visible light and ultrasonic irradiation.

Table 2 indicates that the bacteria survivability decreases with more folate conjugation and minimizes in the Cd-TiO₂/PEG/FA (0.6) sample. This approach is probably related to the tendency of microorganisms to accumulate near the folate sources; therefore as-formed free radicals could easily damage their walls and antibacterial performance of the as-synthesized Cd-TiO₂/PEG/FA compounds improved by increasing the FA to 0.6. Afterward, the antibacterial performance decreased at higher folate content. High amounts of folate may promote its connection to the NPs and cover their surface, as well as intensifying the accumulation of microorganisms around NPs. These events lead to reduce the exposure of light beams (UV or visible light) to the surface of the NPs; therefore the photoexcitation process would be limited.

It should be noted that the antibacterial behavior under ultrasonic irradiation is somewhat different. In this case, the existence of FA led to more decrease in viability (in comparison to the Cd-TiO₂/PEG sample), means that FA molecules cannot prevent ultrasonic waves from reaching NPs. However, the antibacterial performance of the as-synthesized Cd-TiO₂/PEG/FA compound improved via the addition of FA, probably due to the accumulation of bacteria around NPs and facilitating interaction between bacteria and as-formed free radicals.

CONCLUSIONS

Cd-doped TiO₂ NPs were synthesized by a solvothermal assisted sol-gel method. PEG and folic acid as the anti-sedimentation and bait agents were added to the as-synthesized NPs. According to the FTIR results, chemical bonds have been generated between the NPs and PEG molecules and also between Cd-TiO₂/PEG nanocomposite and folic acid molecules. The results of the bactericidal assay pointed out that

the performance of PEG and FA on the antibacterial characteristic was confirmed. PEG plays its role by avoiding agglomeration of the as-synthesized NPs. FA acts as a bait agent for bacteria and led to accumulating them around the NPs. Its efficacy is dose-dependent and maximized at 0.6 weight ratio of FA to Cd-TiO₂. More concentration of FA led to decrease in the antibacterial efficiency under UV or visible light, whereas; it didn't show considerable effect under ultrasonic waves. In comparison to pure Cd-TiO₂ NPs, as-optimized Cd-TiO₂/PEG/FA nanocomposite was more efficacious in bacterial killing especially under ultrasonic irradiation, increasing the diameter of the non-growth halo from 4 to 10 mm.

CONFLICT OF INTEREST

The authors declare that there is no conflict of interests regarding the publication of this manuscript.

REFERENCES

1. Arndt W. Treatment of seed and plants with useful bacteria. Google Patents; 2005.
2. Cole L, Kramer PR. Bacteria, Virus, Fungi, and Infectious Diseases. Human Physiology, Biochemistry and Basic Medicine: Elsevier; 2016. p. 193-6.
3. Moudgil P, Bedi JS, Moudgil AD, Gill JPS, Aulakh RS. Emerging issue of antibiotic resistance from food producing animals in India: Perspective and legal framework. Food Reviews International. 2017;34(5):447-62.
4. Hameed ASH, Karthikeyan C, Ahamed AP, Thajuddin N, Alharbi NS, Alharbi SA, et al. In vitro antibacterial activity of ZnO and Nd doped ZnO nanoparticles against ESBL producing Escherichia coli and Klebsiella pneumoniae. Scientific Reports. 2016;6(1).
5. Jung WK, Koo HC, Kim KW, Shin S, Kim SH, Park YH. Antibacterial Activity and Mechanism of Action of the Silver Ion in Staphylococcus aureus and Escherichia coli. Applied and Environmental Microbiology. 2008;74(7):2171-8.
6. Kubacka A, Diez MS, Rojo D, Bargiela R, Ciordia S, Zapico I, et al. Understanding the antimicrobial mechanism of TiO₂-based nanocomposite films in a pathogenic bacterium. Scientific Reports. 2014;4(1).
7. Jin-hui Z. Research on UV/TiO₂ Photocatalytic Oxidation of Organic Matter in Drinking Water and Its Influencing Factors. Procedia Environmental Sciences. 2012;12:445-52.
8. Guo C, Wang K, Hou S, Wan L, Lv J, Zhang Y, et al. H₂O₂ and/or TiO₂ photocatalysis under UV irradiation for the removal of antibiotic resistant bacteria and their antibiotic resistance genes. Journal of Hazardous Materials. 2017;323:710-8.
9. Zhang Y, Zhou L, Zhang Y. Investigation of UV-TiO₂ photocatalysis and its mechanism in Bacillus subtilis spore inactivation. Journal of Environmental Sciences. 2014;26(9):1943-8.
10. Naghibi S, Vahed S, Torabi O, Jamshidi A, Golabgir MH. Exploring a new phenomenon in the bactericidal response

- of TiO₂ thin films by Fe doping: Exerting the antimicrobial activity even after stoppage of illumination. *Applied Surface Science*. 2015;327:371-8.
11. Moradi V, Jun MBG, Blackburn A, Herring RA. Significant improvement in visible light photocatalytic activity of Fe doped TiO₂ using an acid treatment process. *Applied Surface Science*. 2018;427:791-9.
 12. Ubonchonlakate K, Sikong L, Saito F. Photocatalytic disinfection of *P.aeruginosa* bacterial Ag-doped TiO₂ film. *Procedia Engineering*. 2012;32:656-62.
 13. Dahlan D, Md Saad SK, Berli AU, Bajili A, Umar AA. Synthesis of two-dimensional nanowall of Cu-Doped TiO₂ and its application as photoanode in DSSCs. *Physica E: Low-dimensional Systems and Nanostructures*. 2017;91:185-9.
 14. Naghibi S, Gharagozlou M. Solvothermal Synthesis of M-doped TiO₂ Nanoparticles for Sonocatalysis of Methylene Blue and Methyl Orange (M = Cd, Ag, Fe, Ce, and Cu). *Journal of the Chinese Chemical Society*. 2017;64(6):640-50.
 15. Naghibi S, Madaah Hosseini HR, Faghihi Sani MA, Shokrgozar MA, Mehrjoo M. Mortality response of folate receptor-activated, PEG-functionalized TiO₂ nanoparticles for doxorubicin loading with and without ultraviolet irradiation. *Ceramics International*. 2014;40(4):5481-8.
 16. Yang S-J, Lin F-H, Tsai K-C, Wei M-F, Tsai H-M, Wong J-M, et al. Folic Acid-Conjugated Chitosan Nanoparticles Enhanced Protoporphyrin IX Accumulation in Colorectal Cancer Cells. *Bioconjugate Chemistry*. 2010;21(4):679-89.
 17. Porta F, Lamers GEM, Morrhayim J, Chatzopoulou A, Schaaf M, den Dulk H, et al. Folic Acid-Modified Mesoporous Silica Nanoparticles for Cellular and Nuclear Targeted Drug Delivery. *Advanced Healthcare Materials*. 2012;2(2):281-6.
 18. Zhang J, Rana S, Srivastava RS, Misra RDK. On the chemical synthesis and drug delivery response of folate receptor-activated, polyethylene glycol-functionalized magnetite nanoparticles. *Acta Biomaterialia*. 2008;4(1):40-8.
 19. Dolgonos A, Mason TO, Poeppelmeier KR. Direct optical band gap measurement in polycrystalline semiconductors: A critical look at the Tauc method. *Journal of Solid State Chemistry*. 2016;240:43-8.
 20. Naghibi S, Madaah Hosseini HR, Faghihi Sani MA. Colloidal stability of dextran and dextran/poly ethylene glycol coated TiO₂ nanoparticles by hydrothermal assisted sol-gel method. *Ceramics International*. 2013;39(7):8377-84.
 21. Chowdhuri AR, Tripathy S, Haldar C, Chandra S, Das B, Roy S, et al. Theoretical and experimental study of folic acid conjugated silver nanoparticles through electrostatic interaction for enhance antibacterial activity. *RSC Advances*. 2015;5(28):21515-24.
 22. Margan P, Haghighi M. Hydrothermal-assisted sol-gel synthesis of Cd-doped TiO₂ nanophotocatalyst for removal of acid orange from wastewater. *Journal of Sol-Gel Science and Technology*. 2016;81(2):556-69.
 23. Gharagozlou M, Naghibi S. Surface Modification of TiO₂ Nanoparticles with Vitamin B12: Relationships between Vitamin B12 Content and Its Optical Properties. *Journal of the Chinese Chemical Society*. 2015;62(12):1128-36.
 24. Mahmood L. The metabolic processes of folic acid and Vitamin B12 deficiency. *Journal of Health Research and Reviews*. 2014;1(1):5.
 25. Kavkler K, Gunde-Cimerman N, Zalar P, Demšar A. FTIR spectroscopy of biodegraded historical textiles. *Polymer Degradation and Stability*. 2011;96(4):574-80.
 26. He YY, Wang XC, Jin PK, Zhao B, Fan X. Complexation of anthracene with folic acid studied by FTIR and UV spectroscopies. *Spectrochimica Acta Part A: Molecular and Biomolecular Spectroscopy*. 2009;72(4):876-9.